

## 表示素子用 Poly(diisopropyl fumarate)/E8 複合膜

崔致勳 · 金炳奎<sup>†</sup> · 菊池裕嗣\* · 梶山千里\*

釜山大學校 工科大学 高分子工學科, \*九州大學 工學部 應用物質化學科

(1994년 1월 6일 접수)

### Poly(diisopropyl Fumarate)/E8 Composite Film for Optical Displays

Chi Hoon Choi, Byung Kyu Kim<sup>†</sup>, Hirotsugu Kikuchi\*, and Tisato Kajiyama\*

Dept. of Polymer Science and Engineering, Pusan National University, Pusan 609-735, Korea

\*Dept. of Chemical Science and Technology, Faculty of Engineering, Kyushu University, Fukuoka 812, Japan

(Received January 6, 1994)

**요 약 :** 표시소자로서 응용이 가능할 것으로 짐작되는 고분자/액정 복합막을 다양한 조성에 걸쳐 용매증발법으로 제조하였으며, 막조성, 인가전압과 주파수 및 온도가 복합막의 전기광학적 특성에 미치는 영향을 체계적으로 연구하였다. 아울러 DSC 및 X-ray 회절장치를 이용하여 복합막의 상전이 온도 및 director 배향을 조사하였다. 복합막의 문턱전압은 조성에 관계없이 25 V<sub>pp</sub> 부근이었으며, 액정함량이 증가할수록 rise time은 감소하였다.

**Abstract :** Polymer/LC composite films of various compositions, potentially applicable for optical displays, have been prepared from poly(diisopropyl fumarate)(PDF) and E8 by solvent casting. Effects of film composition, applied electric voltage and frequency, and temperature on the electro-optic performance are reported. In addition, phase transition temperature and orientation changes in the composite have been studied using DSC and X-ray diffractometer, respectively. Threshold voltages of PDF/E8 composite films were around 25 V<sub>pp</sub> independent of composition. Rise time decreased with increasing LC content.

## INTRODUCTION

Recently, there has been an increasing interest in the use of polymer/liquid crystal(LC) composite film in the area of liquid crystal display(LCD). This film is commonly called as polymer dispersed liquid crystal(PDLC) and is applicable for a wide range of areas including displays, switchable windows and other light shutter devices.<sup>1~5</sup>

The operating principle of polymer/LC composite films is based on the reversible operations between light scattering(unpowered) and light transmittance(powered). Consequently, immiscibility of polymer with LC is a prerequisite for light scatter-

ing, which can be induced by two basic techniques, i.e., phase separation and encapsulation. Phase separation technique is again divided into three, viz., polymerization induced phase separation(PIPS), thermally induced phase separation(TIPS), and solvent induced phase separation(SIPS).<sup>6~10</sup>

This work is a continuation of our earlier works<sup>11</sup> which were confined to a specific film composition and limited measurements. We have prepared poly(diisopropyl fumarate)/E8 composite film in a wide range of film composition using a SIPS technique. The effects of polymer/LC composition, applied voltage, frequency, and temperature on elec-

tro-optic properties were investigated. In addition, phase transition temperature and change in orientation were also studied using a differential scanning calorimeter(DSC) and an X-ray diffractometer.

## EXPERIMENTAL

The liquid crystal(LC) material used in this study was E8, which is a commercial nematic LC mixture with positive dielectric anisotropy, and polymer matrix is poly(diisopropyl fumarate) (PDF). Table 1 lists the detailed characteristics of the materials used.

PDF and LC in desired proportions were dissolved in chloroform at room temperature. The homogenized solutions were then poured on a PET film. For electro-optic measurements, the cells were prepared by sandwiching the composite film between two indium-tin oxide(ITO)-coated glass plates. Electro-optic properties were measured using our lined-up facilities described earlier.<sup>2,11</sup>

To observe the aggregation structure of the composite film, LC phase was extracted in methanol for 10 h at room temperature. Morphology was studied using a scanning electron microscope (SEM, Hitachi S-430) from the fractured surface (in liquid nitrogen), which was subsequently sput-

tered with gold before viewing.

Thermal properties of the films were determined from 200 K to 400 K using a differential scanning calorimeter(DSC). The composite films were sealed in DSC pan with a crimping and welding press. The DSC thermograms were taken at a heating rate of 10 K/min.

X-ray diffraction photographs were taken using an X-ray diffractometer. Quartz was used as a reference sample to calculate Bragg spacing. For X-ray measurements, PDF film and PDF/LC composite film were laminated to 3 mm in thickness while LC was filled into a container. Irradiation time, voltage, current, and camera length were 3 h, 50 kV, 200 mA, and 65.54 mm, respectively.

## RESULTS AND DISCUSSION

**Morphology.** In SIPS, phase morphology is governed by a number of factors such as type of solvent, solvent evaporation rate, casting temperature, and polymer/LC composition.<sup>2,3,12</sup> The phase morphologies of PDF/E8 composite films are shown in Fig. 1. In PDF-rich composition ( $\geq 60$  wt % PDF), E8 formed isolated spherical domains, less than  $0.5\mu\text{m}$  in diameter, and the morphology is non-uniform along the thickness direction due to the rapid evaporation and solidification near the air facing surface.<sup>12</sup> However, as the content of LC increases, liquid crystal domains are interconnected to form co-continuous structure. This interconnected structure results in strong light scattering of the unpowered films.<sup>2</sup> The LC domain size is larger in E8-rich than in PDF-rich films.

**Electro-Optic Properties.** Fig. 2 shows transmittance as a function of the applied voltage. Transmittance shows a minimum at 60 wt% LC both for powered and unpowered ( $V_{\text{pp}}=0$ ) films. Light scattering in off-state is also caused by the spatial distortion of nematic directors in curved LC channels as well as refractive index mismatching between polymer matrix and LC.<sup>13,14</sup> Consequently, the degree of light scattering depends strongly on the film morphology. SEM micrographs suggest

**Table 1.** Characteristics of Materials Used in the Experiment

Materials	Characterics	Producer
Poly(diisopropyl fumarate)(PDF)	$n=1.464$	Nippon Oil & Fat
	$M_w=2.45 \times 10^5$	
	$T_g \sim 500 \text{ K}$ (decomposition)	
E8	$n_i=1.774$	BDH
	$n_e=1.527$	
	$\eta(298^\circ\text{F})=54\text{cPs}$	
	$T_{\text{KN}}=261\text{K}$ $T_{\text{NI}}=345\text{K}$	
Chloroform	$d=1.492$	Aldrich
	$b_p=334\text{K}$	
	$\text{FW}=119.38$	



Fig. 1. SEM micrographs of PDF/E8 composite films cast at different LC weight fraction : (a) PDF/E8(80/20), (b) PDF/E8(60/40), (c) PDF/E8(40/60).

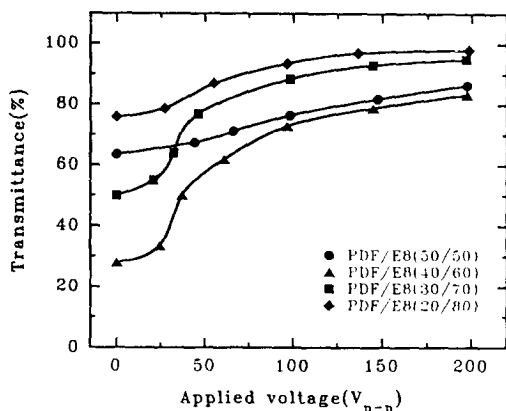


Fig. 2. Transmittance as a function of applied voltage (1 kHz, 293 K,  $11\mu\text{m}$ ).

that co-continuous structure should give film higher light scattering, and maximum light contrast is obtained at 40/60 composition. The threshold voltages of the films are observed at about  $25 V_{p-p}$ . The transmittance increases with voltage up to  $150 V_{p-p}$ , beyond which it is almost independent on the applied voltage, indicating that the director orientation is almost completed at  $150 V_{p-p}$ , and transmittance reaches its maximum.<sup>14</sup>

Rise time ( $\tau_R$ ) of the films are shown in Fig. 3. At lower voltage ( $\leq 100 V_{p-p}$ ), rise time decreases rapidly and at higher voltage ( $\geq 150 V_{p-p}$ ) it decreases slowly with voltage. It is generally accepted that the shape and size of LC domains can be a significant factor to control the response time.<sup>6</sup> As the LC content increases, droplet size increases, the total interfacial area decreases and thus LC

molecules could easily be oriented toward the external field to make rise time short.<sup>3</sup> In conventional nematic liquid crystal cells, reciprocal rise time is proportional to the square of applied voltage.<sup>6</sup> Rise time-voltage relationship can be seen more clearly in a full logarithmic plot of  $\tau_R$  vs.  $V_{p-p}$  (Fig. 4). The straight lines drawn are the linear least square fits to the experimental data at each composition. For all of the compositions, the slopes of the straight lines are about  $-2$ . This is well agreed with theoretical value.<sup>6,15</sup>

Fig. 5 shows transmittance as a function of frequency, where transmittance increases smoothly with frequency. This frequency dependence is probably due to the dielectric loss in low frequency region. In polymer/LC composite films, the external field is distributed into polymer and LC

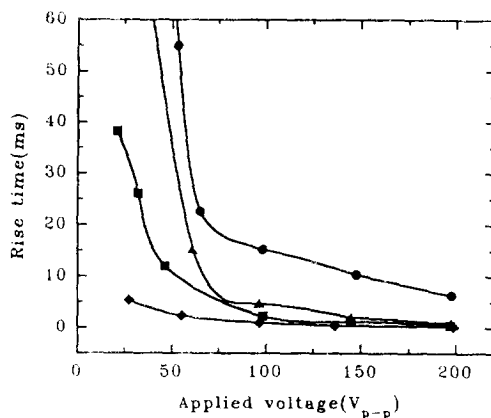


Fig. 3. Rise time as a function of applied voltage (1 kHz, 293 K,  $11\mu\text{m}$ ). Same symbols as in Fig. 2.

domains. The electric field distribution on LC and polymer phase ( $E_{LC}/E_P$ ) is given as :<sup>3,14</sup>

$$\frac{E_{LC}}{E_P} = \frac{|\epsilon_P^*|}{|\epsilon_{LC}^*|} = \left( \frac{\omega^2 \epsilon_P'^2 + \sigma_P^2}{\omega^2 \epsilon_{LC}'^2 + \sigma_{LC}^2} \right)^{1/2}$$

where  $E$ ,  $\epsilon^*$ ,  $\omega$ ,  $\epsilon'$ , and  $\sigma$  are applied electric field, complex dielectric constant, angular frequency, dielectric constant and conductivity, respectively. From this equation it is seen that at low enough frequency,  $E_{LC}/E_P$  is inversely proportional to the conductivity ratio and at high enough frequency to the dielectric constant ratio. However, these two

ratios are not exactly the same and hence there should occur interfacial polarizations as the electric frequency decreases from dielectric to conductive region. Therefore,  $E_{LC}/E_P$  is frequency dependent, and transmittance decreases due to the decrease of  $E_{LC}/E_P$  as frequency decreases.

Fig. 6 shows rise time as a function of frequency. As expected, rise time decreases with frequency because  $E_{LC}/E_P$  is increased with frequency. This effect is more pronounced at frequencies below 100 Hz.

Fig. 7 shows the transmittance as a function of temperature. In the absence of external field, the transmittance increases with increasing temperature up to the  $T_{NI}$  (nematic-to-isotropic transition temperature) of LC. This increased transmittance is caused by the decreased birefringence ( $\Delta n = n_{||} - n_{\perp}$ ) of LC.<sup>13</sup> At and above  $T_{NI}$ , the transmittance is over 90% and independent of temperature since the mismatch of refractive indices between polymer and isotropic value of LC is small and independent of temperature. It is further seen that the constant transmittance above  $T_{NI}$  increases with LC content due to the decreased number of scattering centers (interfaces).

Rise time decreases with temperature (Fig. 8), however, the tendency is not significant except 50/50 composition where the LC forms dispersed droplets rather than the co-continuous ones of hi-

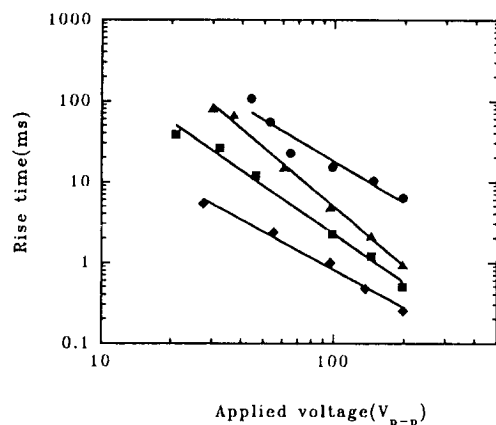


Fig. 4. Log-log plot for rise time vs. applied voltage. Same symbols as in Fig. 2.

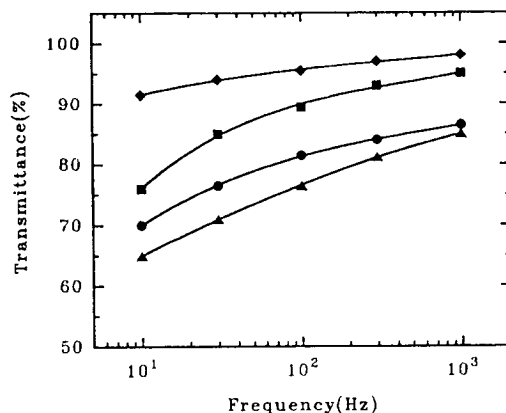


Fig. 5. Transmittance as a function of applied frequency (200 V<sub>p-p</sub>, 293 K, 11μm). Same symbols as in Fig. 2.

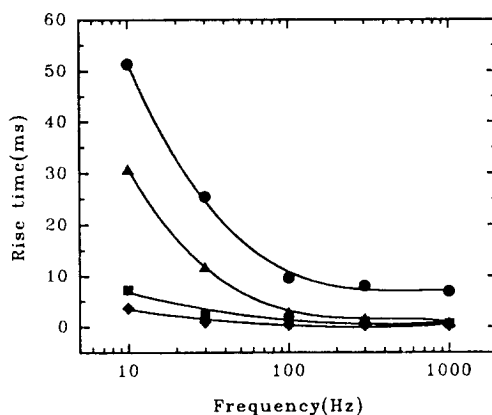


Fig. 6. Rise time as a function of applied frequency (200 V<sub>p-p</sub>, 293 K, 11μm). Same symbols as in Fig. 2.

gher LC contents. The decrease of rise time with temperature is mainly due to the increased mobility of LC molecules at elevated temperature.

**Thermal Properties.** Fig. 9 shows DSC thermograms of PDF, E8, and PDF/E8 composite films. The  $\beta$ -transition temperature of PDF is 340 K,<sup>16</sup> and  $T_{KN}$ (crystal-to-nematic transition temperature) and  $T_{NI}$  of E8 are 261 K and 345 K, respectively. The  $\beta$ -transition temperature of PDF in PDF/E8 composite films is about 324 K, which is lower than that of pure PDF by 15 K. The decrease of  $\beta$ -transition temperature indicates that LCs act as plasticizers for PDF. On the contrary,  $T_{NI}$  is so-

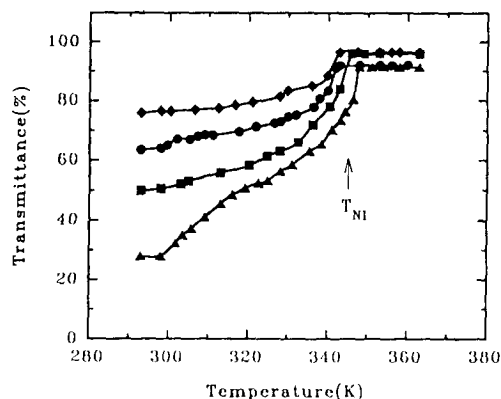


Fig. 7. Transmittance as a function of temperature in the absence of external field(11 $\mu$ m). Same symbols as in Fig. 2.

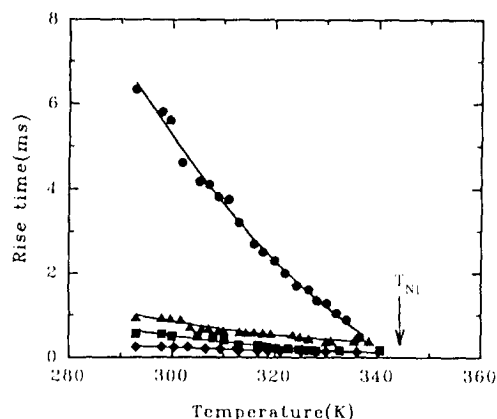


Fig. 8. Rise time as a function of temperature(1 kHz, 200 V<sub>pp</sub>, 11 $\mu$ m). Same symbols as in Fig. 2.

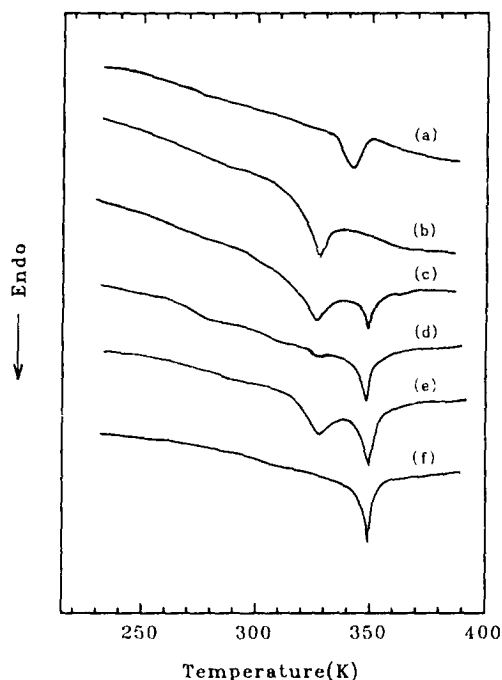
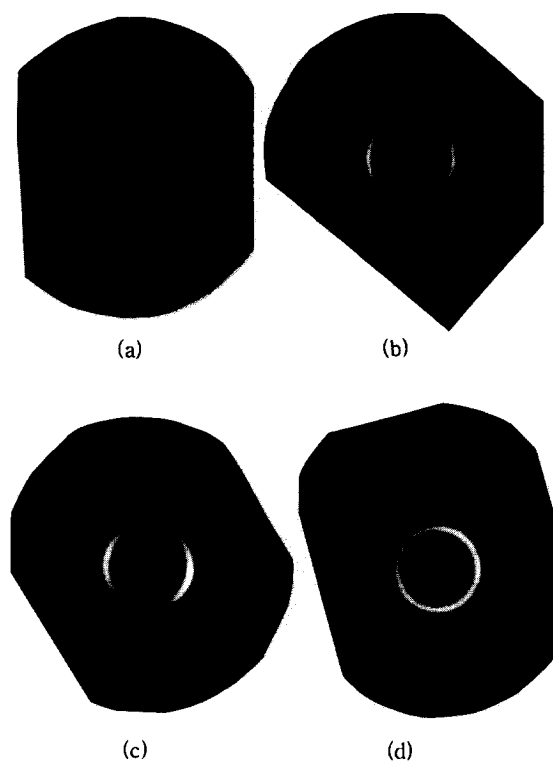


Fig. 9. DSC thermograms for PDF/E8 composite films : (a) PDF, (b) PDF/E8(80/20), (c) PDF/E8(60/40), (d) PDF/E8(40/60), (e) PDF/E8(20/80), (f) E8.

mewhat increased in the composite. This tendency is likely due to the selective dissolution of lower  $T_{NI}$  component of E8 into PDF. It is noted that the commercially available LCs including E8 are eutectic mixtures because single compound has limited nematic temperature range.

**X-ray Diffraction.** Fig. 10 shows X-ray diffraction photographs for PDF, E8, and PDF/E8 composite film. X-ray diffraction photograph for E8(Fig. 10.a) simply shows two diffuse rings. Diffraction photograph for PDF(Fig. 10.b) shows two rings. Stronger one corresponds to Bragg spacing,  $d_b = 1.13$  nm, whereas weaker one(diffuse ring) to  $d_b = 0.47$  nm.<sup>17</sup> Diffraction photographs for PDF/E8 composite film(Fig. 10.c and d) show neither sign of PDF crystallinity nor induced smectic orientation of E8, although there appear a kind of orientation in Fig. 10.a and c. Since the diffraction pattern is not changed as compared to that of pure components, one can infer that there might be no structural change in molecular level.



**Fig. 10.** X-ray diffraction photographs : (a) E8, (b) PDF, (c) PDF/E8(40/60), edge view (d) PDF/E8(40/60), through view.

## REFERENCES

1. G. P. Montgomery, *Proc. SPIE vol. IS4*, 577 (1989).
2. A. Miyamoto, H. Kikuchi, Y. Morimura, and T. Kajiyama, *New Polymeric Mater.*, **2**, 1 (1990).
3. B. K. Kim and Y. S. Ok, *J. Appl. Polym. Sci.*, **49**, 1769 (1993).
4. S. C. Jain and D. K. Rout, *J. Appl. Phys.*, **70**, 6988 (1991).
5. J. Ding and Y. Yang, *Jpn. J. Appl. Phys.*, **31**, 2837 (1992).
6. J. W. Doane in "Liquid Crystals-Applications and Uses", edited by B. Bahadur, Vol. 1, World Scientific, Singapore, 1990.
7. P. S. Drazalic, *J. Appl. Phys.*, **60**(6), 2142 (1986).
8. J. L. Fergason, U. S. Patent 4,616,903 (1986).
9. J. L. West, *Mol. Cryst. Liq. Cryst.*, **157**, 427 (1988).
10. L. L. Chapoy, "Recent Advances in Liquid Crystalline Polymers", Elsevier Science, New York, 1986.
11. C. H. Choi, Y. S. Ok, B. K. Kim, W. J. Cho, Y. J. Shin, and T. Kajiyama, *Polymer(Korea)*, **15**(6), 709 (1991).
12. H. Strathmann in "Handbook of Industrial Membrane Technology", edited by M. C. Porter, Noyes Publication, New Jersey, 1990.
13. N. A. Vaz and G. P. Montgomery, Jr., *J. Appl. Phys.*, **62**(8), 3161 (1987).
14. A. Miyamoto, H. Kikuchi, S. Kobayashi, Y. Morimura, and T. Kajiyama, *Macromolecules*, **24**(13), 3915 (1991).
15. M. Mucha, *J. Appl. Polym. Sci.*, **43**, 175 (1991).
16. K. Yamada and M. Takayanagi, *Polymer*, **27**, 1054 (1986).
17. M.S. Cortizo, E.M. Macchi, and R.V. Figini, *Polymer Bulletin*, **19**, 477 (1988).